Statistical Local Effect of Synoptic-Scale Transient Eddies on the Time-Mean Flow in the Northern Extratropics in Winter

EERO HOLOPAINEN

Department of Meteorology, University of Helsinki, Hallituskatu 11–13, 00100 Helsinki 10, Finland

(Manuscript received 8 February 1984, in final form 5 June 1984)

ABSTRACT

Time-filtered grid-point data for the northern extratropics in winter have been used to study the local effect on the time-mean flow, arising from the "synoptic-scale" transient eddies (TE), which have periods between 2.5 and 6 days. The local TE effect is defined as the net work done on the time-mean flow by the TE induced force. In the interior of an air column, this force is determined by the irrotational TE flux of quasi-geostrophic potential vorticity; at the upper and lower boundaries, it is determined by the irrotational TE heat flux. The net work in the entire air column consists of the sum of a "baroclinic" part, which affects only the vertical shear of the time-mean flow, and of a "barotropic" part, which affects mainly the vertically-averaged component of the time-mean flow.

The results show that the baroclinic part of the net TE work dominates and, in the storm track regions, gives an energy conversion from the time-mean flow to the synoptic-scale eddies. The barotropic part of the TE work shows in these same regions a partially compensating conversion of the TE energy back to the mean flow. These eddies thus tend to dissipate the baroclinic component and to strengthen the barotropic component of the time-mean flow with the concomitant tendency of strengthening the surface westerlies in the storm track regions and of shifting the time-mean jet stream polewards.

The "energy method" introduced in the present paper for the description of the interplay between the time-mean flow and the transient eddies is compared with other methods suggested in the literature for this purpose. The effect of synoptic-scale eddies on the time-mean flow is further compared briefly with that exerted by low-frequency fluctuations with periods between 10 and 90 days.

1. Introduction

The dynamic effect of the atmosphere's transient variability ("large-scale turbulence") on the time-mean flow is complicated. This complexity is, in part, due to the fact that the transient eddies (TE) do not arise from a narrow frequency band with specific dynamics, but from a continuous spectrum of fluctuations, with different parts of the spectrum having different dynamics and strong nonlinear interactions with other parts. A further reason for this complexity is the fact that the net effects on the time-mean flow, arising from the TE in a certain frequency band, are determined not only by the relevant TE flux divergence terms but also by the effect of the secondary circulations induced by these eddies. While the TE fluxes and their divergences can, in principle, be easily calculated from observations (e.g., Lau and Wallace, 1979; Lau *et al.*, 1981; Oort, 1983), the effect of the TE induced secondary circulations is more difficult to estimate.

In recent studies by Holopainen *et al.* (1982; hereafter referred to as A) and Holopainen (1983), the net local effect of TE on the time-mean flow was depicted with the aid of a force vector, which is determined by the irrotational TE flux of quasi-geostrophic potential vorticity. It was shown in A that the TE tend to dissipate the potential enstrophy of the time-mean (i.e., stationary) eddies, and that the main role in this rather efficient dissipation (time scale of 4–5 days) is played by the long-period (10–90 days) fluctuations.

Lau and Holopainen (1984; hereafter referred to as B) illustrate the net local TE effect with the aid of initial isobaric height tendencies, which arise in a quasi-geostrophic model atmosphere if the TE fluxes of heat and momentum are switched on. This method of illustrating the TE effects is an extension into three dimensions of Pfeffer's (1981) work on the net eddy effects in the mean meridional plane. It takes into account both the direct effect of the TE fluxes and the indirect effect of the TE induced secondary circulations and guarantees that the response satisfies the hydrostatic and geostrophic balance requirements. The results for the synoptic-scale eddies (i.e., eddies having periods between 2.5 and 6 days) vividly demonstrate (Fig. 3 in B) how, in storm track regions, the TE heat fluxes tend to weaken the baroclinic component of the time-mean flow; whereas, the vorticity fluxes tend to strengthen the barotropic component of the time-mean flow.

The present paper reports on a continuation of the

research described in A and B. The data used here are the same as in B. In A and B, the TE effects were considered without any attention given to the properties of the mean flow. In this paper, however, a new method for measuring the local interplay between the time-mean flow and the transient eddies is formulated, and the new interaction terms depend not only on eddy variances and covariances, but also on the structure of the mean flow.

We will deal here mainly with the effects of synoptic-scale eddies on the climatological time-mean flow. This may appear strange in light of the results reported in A, showing that the main effects on mean flow arise from the long-period fluctuations. This emphasis can be justified, however, by arguing that in the future, in models of the atmosphere's large-scale behavior, we may be able to account explicitly for the long-period variability, while the effects of the synoptic-scale eddies are considered only in a statistical sense. The present study on the interactions between the synoptic-scale eddies and the climatological mean flow may also indicate the nature of the effects of such eddies in a more interesting case: that in which the "mean" flow consists of the climatological mean together with the long-period fluctuations and, thus, varies slowly with time.

In Section 3, some traditional energy considerations relevant to our problem are first presented. A new method for measuring the local rate of energy conversion from the mean flow energy to the TE energy is then formulated and its spatial distribution estimated using time-filtered circulation data (described in Section 2). In Section 4, this new concept is compared with other ways of depicting the TE effects. Finally, in Section 5, some points are made on the results obtained using the new concepts to estimate the effect of long-period (10–90 days) fluctuations on the climatological mean flow.

2. Data

The observational data set of this study is the same as in B. It was first used by Blackmon (1976) and consists of the Northern Hemisphere circulation statistics, computed from twice-daily gridded analyses produced operationally by the U.S. National Meteorological Center (NMC) during an eight-winter period (1966/67 to 1968/69, 1970/71 to 1974/75). The winter season is taken to be the 120-day period starting 15 November. In order to distinguish between transient phenomena of various time scales, the statistics have been compiled using time series obtained by applying the following time-filters:

- A band-pass (BP) filter retaining fluctuations that have periods between 2.5 and 6 days. In this paper, these fluctuations are called synoptic-scale transient eddies and receive the main attention.
- A low-pass (LP) filter retaining fluctuations that have periods between 10 and 90 days.

The filtering procedures have been described by Blackmon (1976). The NMC circulation statistics have been documented in detail by Lau *et al.* (1981).

3. The local interplay between the synoptic-scale transient eddies and the time-mean flow

Some estimates based on the traditional concepts of energy conversion between the time-mean flow and the TE are first discussed. These concepts have an unambiguous interpretation only when the whole atmosphere is considered, and do not necessarily provide much insight into the local TE–mean flow interplay. For this reason, a possibly more useful framework is introduced in Section 3b.

a. Some traditional energy considerations

The temporal variances of temperature and wind are local measures of the TE activity. Instead of these variances, we may speak of TE available potential energy a_{TE} in an air column:

$$a_{TE} = \frac{1}{2}\int_0^{p_0} c_p \gamma \overline{T'^2}\,\frac{dp}{g}, \tag{1}$$

and the corresponding kinetic energy k_{TE}:

$$k_{TE} = \frac{1}{2}\int_0^{p_0} \overline{\mathbf{V}'^2}\,\frac{dp}{g}. \tag{2}$$

In these expressions, T denotes temperature, c_p the specific heat at constant pressure, γ a stability factor (function of pressure only), $\mathbf{V} = u\mathbf{i} + v\mathbf{j}$, the horizontal wind vector and p_0 the surface pressure; an overbar denotes time-average and a prime denotes a deviation from the time average. [The concept of available potential energy, as originally formulated by Lorenz (1955), is valid only for the global atmosphere. We may, however, interpret a_{TE} in (1) as a local TE contribution to the time-averaged global available potential energy.]

By using filtered data for calculating the variances in (1) and (2), the contributions to a_{TE} and k_{TE} from that frequency band which is associated with the filter used can be estimated. All the quantities obtained by using the band-pass filtered data (periods 2.5–6 days) will be denoted in the following by a superscript BP.

Figure 1 shows the distribution of a_{TE}^{BP} and k_{TE}^{BP} in the 100–1000 mb layer. Perhaps the most striking feature in this figure is the similarity of the two patterns, which indicates a tendency to an equipartitioning of energy between the available potential energy and kinetic energy. The energy maxima are found off the eastern coasts of the two continents and can be used to define the two major storm tracks.

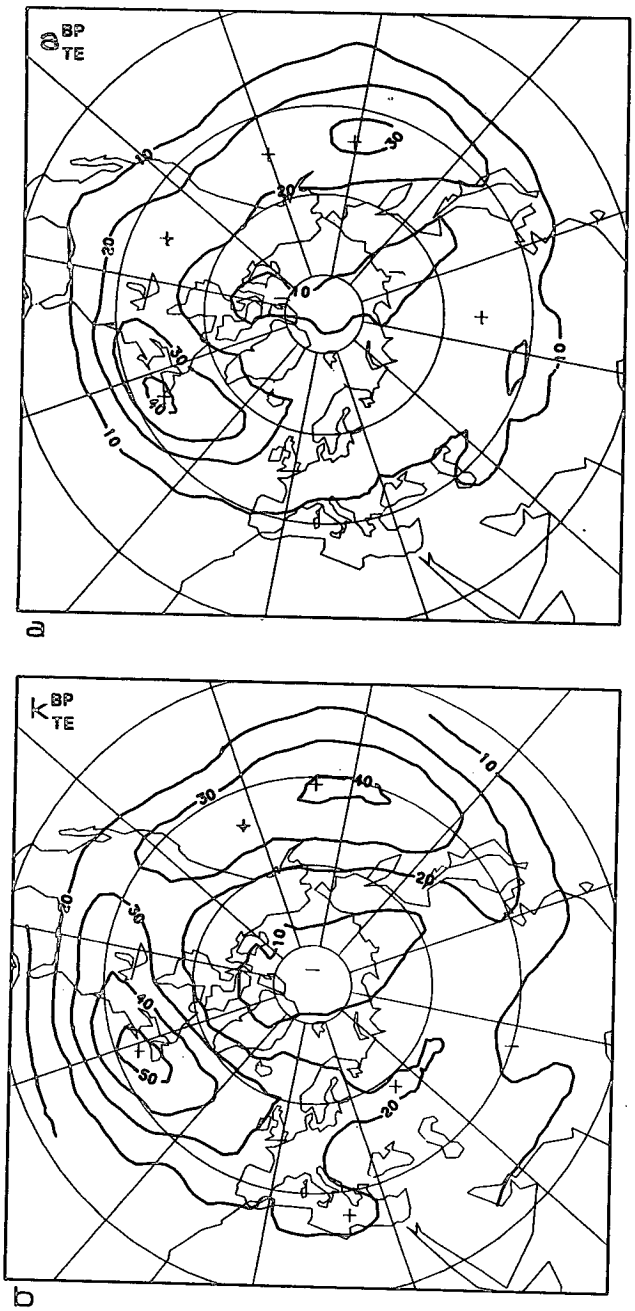

FIG. 1. Distribution of the (a) available potential energy a_{TE}^{BP} and (b) kinetic energy k_{TL}^{BP}, averaged over the 100–1000 mb layer, in the band-pass eddies in winter. Units: J kg^{-1}.

In this study, we are not concerned with the budgets of a_{TE}^{BP} and k_{TE}^{BP} but only with the interactions between the band-pass synoptic eddies and the time-mean flow. The traditional expressions for the energy conversion from the time-mean flow to the transient eddies can be found, e.g., in Oort (1964; Appendix B). A contribution of a local air column to these global integrals is, when only the effects of horizontal TE fluxes are considered, given by

$$\mathrm{CA} = -\int_0^{p_0} c_p \gamma \overline{T'\mathbf{V}'} \cdot \nabla \bar{T} \frac{dp}{g}, \tag{3}$$

$$\mathrm{CK} = -\int_0^{p_0} \left\{ \frac{\overline{u'u'}}{a\cos\phi}\frac{\partial \bar{u}}{\partial \lambda} + \overline{u'v'}\cos\phi \frac{\partial}{a\partial\phi}\left(\frac{\bar{u}}{\cos\phi}\right) + \frac{\overline{u'v'}}{a\cos\phi}\frac{\partial \bar{v}}{\partial\lambda} + \overline{v'v'}\frac{\partial \bar{v}}{a\partial\phi} - \overline{u'u'}\bar{v}\frac{\tan\phi}{a} \right\} \frac{dp}{g}. \tag{4}$$

In these expressions, λ and ϕ denote the longitude and latitude, respectively, a the radius of the earth and ∇ the del operator at constant pressure level. The expression for CA is positive when the TE receives energy from the mean flow; similarly, CK is positive when kinetic energy is converted from the mean flow to the transient eddies. Here CK can be written approximately as [Simmons *et al.*, 1983; Eq. (5)]

$$\mathrm{CK} = -\int_0^{p_0} \left\{ (\overline{u'^2} - \overline{v'^2})\frac{\partial \bar{u}}{\partial x} - \overline{u'v'}\frac{\partial \bar{u}}{\partial y} \right\} \frac{dp}{g}. \tag{4'}$$

The contributions by the band-pass transient eddies to the expressions (3) and (4), denoted as CA^{BP} and CK^{BP}, are shown in Fig. 2. The values of CA^{BP} are positive almost everywhere, with the area-averaged value being 1.0 W m^{-2} (1000 mb)$^{-1}$ and particularly large in the vicinity of the storm tracks. (The storm tracks are marked by thick arrows with dashed shafts in Figs. 2 and 3.) The pattern of CA^{BP} thus indicates an energy input from the mean flow to the band-pass transient eddies. As these eddies are known to have large downgradient heat fluxes across the storm tracks (e.g., Lau *et al.*, 1981) it is natural to find the maxima of CA^{BP} in these regions.

While CA^{BP} is positive almost everywhere, the sign of CK^{BP} (Fig. 2b) has great variation geographically; therefore, its area-average (−0.1 units) is only a small residual resulting from relatively large local contributions. The large longitudinal variation of CK^{BP} appears to arise mainly from the first term in (4′). In the jet exit regions over the oceans, where $\partial\bar{u}/\partial x < 0$, one finds $\mathrm{CK}^{BP} < 0$ because in the band-pass eddies $\overline{v'^2} > \overline{u'^2}$ (e.g., Hoskins *et al.*, 1983).

In the pattern of CK^{BP} it is difficult to see any clear association with the storm tracks. This may be due to the terms CK^{BP}, and also CA^{BP}, not being the best indicators of how the local time-mean flow is affected by the synoptic-scale eddies. There are alternative ways to write the equations for the TE energetics (Holopainen, 1978; Plumb, 1983). These alternatives are formally connected with the fact that in the budget equations of mean flow energy, there are, in addition to the conversion terms CA and CK, some flux divergence terms that contain both TE and

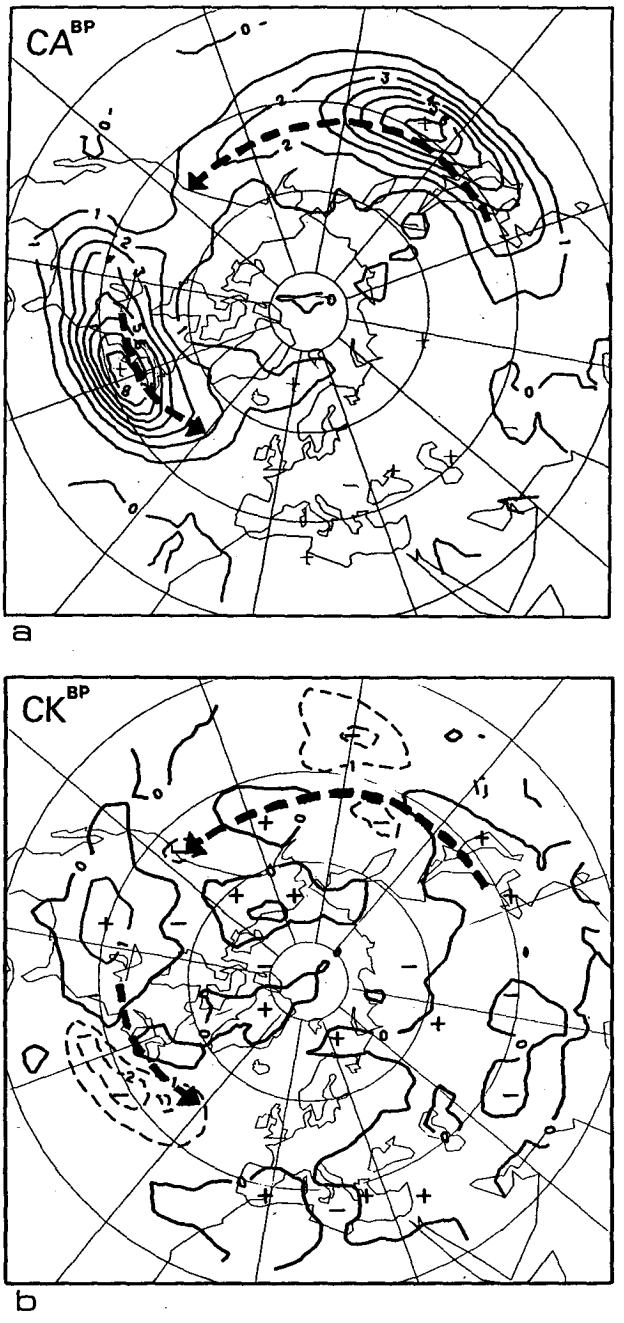

FIG. 2. Distribution of the conversion terms (a) CA^{BP} and (b) CK^{BP}, averaged over the 100–1000 mb layer in the band-pass eddies in winter. Isoline spacing 1 W m^{-2} (1000 mb)$^{-1}$. Positive values (solid isolines) indicate energy conversion from the mean flow to the eddies. Negative values are indicated by dashed isolines. The dashed arrows indicate the two major "storm tracks," identified by the maximum of TE energy $a^{BP}_{TE} + k^{BP}_{TE}$.

mean flow quantities. For this reason, the local TE mean flow interactions are considered in the next section in a framework that is more elaborate than that represented by Eqs. (3) and (4).

b. Local interplay between the synoptic-scale transient eddies and the time-mean flow

Since we are presently interested in the net local effect of the TE on the time-mean flow, we will lump all dynamic TE effects into one single force term. This can be done by taking into account that the most essential dynamics of the large-scale motion systems in the middle and high latitudes are contained in the quasi-geostrophic potential vorticity (QGPV) equation. In the time-averaged QGPV equation, the effect of transient eddies enters only as the TE flux convergence of QGPV. Consequently, in the transformed equations of time-mean motion [e.g., Hoskins, 1983; Eqs. (7.38)–(7.40)], the curl of which gives the time-averaged QGPV equation, the nondivergent time-mean force due to the transient eddies is given by

$$\mathbf{F}_{ND} = (\overline{q'\mathbf{V}'})_D \times \mathbf{k}, \tag{5}$$

where $(\overline{q'\mathbf{V}'})_D$ is the divergent (irrotational) component of the TE flux of QGPV (the subscripts D and ND refer to the divergent and nondivergent components, respectively) and $\mathbf{k}$ is the unit vector in the vertical. The nondivergent flux component $(\overline{q'\mathbf{V}'})_{ND}$ has relatively little importance, because it enters only the time-averaged divergence equation, where its relative magnitude is small compared to the terms arising from the pressure gradient and Coriolis forces.

As shown in A, the force $\mathbf{F}_{ND}$ can be written as the sum of two terms:

$$\mathbf{F}_{ND} = \mathbf{F}^{VORT}_{ND} + \mathbf{F}^{HEAT}_{ND}, \tag{6}$$

where

$$\mathbf{F}^{VORT}_{ND} = (\overline{\zeta'\mathbf{V}'})_D \times \mathbf{k},$$

(ζ denotes relative vorticity), and can also be evaluated as the nondivergent component of the vector

$$\mathbf{A}_H = \left(-\frac{1}{a\cos\phi}\frac{\partial}{\partial\lambda}\overline{u'u'} - \frac{1}{a\cos\phi}\frac{\partial}{\partial\phi}\overline{u'v'}\cos\phi + \frac{\overline{u'v'}}{a}\tan\phi\right)\mathbf{i} + \left(-\frac{1}{a\cos\phi}\frac{\partial}{\partial\lambda}\overline{u'v'} - \frac{1}{a\cos\phi}\frac{\partial}{\partial\phi}\overline{v'v'}\cos\phi - \frac{\overline{u'u'}}{a}\tan\phi\right)\mathbf{j},$$

$$\mathbf{F}^{HEAT}_{ND} = -f\frac{\partial}{\partial p}\left\{\frac{(\overline{\theta'\mathbf{V}'})_D \times \mathbf{k}}{\tilde{S}}\right\}. \tag{7}$$

In (7), f denotes the Coriolis parameter, θ potential temperature, $S = -\partial\theta/\partial p$ and $\tilde{}$ the horizontal average.

The force $\mathbf{F}^{VORT}_{ND}$ is not subject to any particular vertical boundary conditions. However, the nondivergent TE heat fluxes at the top and bottom boundary impose an important constraint on the vertical average of $\mathbf{F}^{HEAT}_{ND}$. As originally shown by Bretherton (1966)

(see also the discussion in A and in Hoskins, 1983), $\mathbf{F}_{ND}$ can be formally treated as having, due to these boundary heat fluxes, the shape of a delta function at the boundaries such that its vertical average is zero. This implies that $\mathbf{F}_{ND}^{HEAT}$ acts on the baroclinic (shear) part of the time-mean flow and has no effect on the barotropic (i.e., vertically-averaged) part.

The work done by the TE induced force $\mathbf{F}_{ND}$ against the time-mean flow, per unit mass, is given by $\bar{\mathbf{V}}_{ND} \cdot \mathbf{F}_{ND}$. Integrating this expression over the mass of the entire air column, one obtains

$$\int_0^{p_0} \bar{\mathbf{V}}_{ND} \cdot \mathbf{F}_{ND} \frac{dp}{g} = \int_0^{p_0} \bar{\mathbf{V}}_{ND} \cdot \mathbf{F}_{ND}^{VORT} \frac{dp}{g} + R \int_0^{p_0} (\tilde{\bar{S}}p)^{-1} (\overline{\theta'\mathbf{V}'})_D \cdot \nabla \bar{T} \frac{dp}{g} - \frac{f}{g} \frac{[\bar{\mathbf{V}}_{ND} \times (\overline{\theta'\mathbf{V}'})_D] \cdot \mathbf{k}}{\tilde{\bar{S}}} \Big|_{p=p_0} . \quad (8)$$

In (8), we can move the third term on the rhs to the lhs and interpret it formally as the work done by $\mathbf{F}_{ND}^{HEAT}$ in the infinitesimally thin sheet at the lower boundary. We may then define the total work done by $\mathbf{F}_{ND}$ (including the contribution of the delta function at the boundary) as

$$C = -\int_0^{p_0} \bar{\mathbf{V}}_{ND} \cdot \mathbf{F}_{ND} \frac{dp}{g} - \frac{f}{g} \frac{(\bar{\mathbf{V}}_{ND} \times (\overline{\theta'\mathbf{V}'})_D) \cdot \mathbf{k})}{\tilde{\bar{S}}} \Big|_{p=p_0} . \quad (9)$$

On the basis of (8), C can be also written as

$$C = C1 + C2, \quad (10)$$

where

$$C1 = -\int_0^{p_0} c_p \gamma (\overline{T'\mathbf{V}'})_D \cdot \nabla \bar{T} \frac{dp}{g}, \quad (11)$$

$$C2 = -\int_0^{p_0} \bar{\mathbf{V}}_{ND} \cdot \mathbf{F}_{ND}^{VORT} \frac{dp}{g} . \quad (12)$$

Positive values of the expressions (10)–(12) indicate a local conversion of the mean flow energy to the TE energy. The term $C1$ is zero when the local baroclinicity of the time-mean flow is zero ($\nabla \bar{T} = 0$). Hence, it may be called the local baroclinic conversion term. Because $\mathbf{F}_{ND}^{VORT}$ appears to have an equivalent-barotropic vertical structure and the main contribution to $C2$ comes from the work done on the vertically-averaged time-mean flow, the term $C2$ could (somewhat less accurately) be called the local barotropic conversion term.

In order to estimate the patterns of $C1$ and $C2$ from the NMC data, several vector fields had to be decomposed into their divergent and nondivergent component fields. This was done by calculating first, for the grid points north of 20°N, the values of the divergence and vorticity of the vector field in question. These fields were then assumed to vanish at the equator and were linearly interpolated between 0 and 20°N. They were then expanded in series of spherical harmonics P_n^m where n is the total wavenumber and m the zonal wavenumber. The potential function (streamfunction) for the divergent (nondivergent) part of the vector field could be obtained by first solving the Poisson equation for each wavenumber and then adding the contributions from different wavenumbers. The results shown in this paper are obtained by adding the contributions from waves for which $m \leqslant 20$ and $n \leqslant 30$.

Figures 3a and b show the distribution of $C1^{BP}$ and $C2^{BP}$, respectively. The pattern of $C1^{BP}$ is seen to be qualitatively similar to the pattern of CA^{BP} in Fig. 2a. This is not surprising in light of the similarity of the expressions (3) and (11), and the fact that the TE heat flux in the band-pass eddies is dominated by the divergent component. The pattern of $C2^{BP}$ in Fig. 3b is entirely different from that of CK^{BP} (Fig. 2b). While CK^{BP} was characterized by large longitudinal variation, the main variability of $C2^{BP}$ is in the meridional direction. The distribution of $C2^{BP}$ becomes understandable in light of the pattern of $\mathbf{F}_{ND}^{VORT}$ for the band-pass eddies (Fig. 6 in A). Over the storm track regions, this force has a large magnitude and is directed eastward, whereas, south from the storm tracks it is directed westward. When such a force is multiplied by $\bar{\mathbf{V}}_{ND}$, which is eastward, one gets from (12) negative values of $C2^{BP}$ (i.e., a barotropic energy conversion from the eddies to the mean flow) over the storm tracks, and positive values south of them. Because maximum mean wind also occurs south of the storm tracks, we note that the barotropic processes in the synoptic-scale eddies effectively tend to shift the mean jet stream polewards. Such an effect of the eddies on the zonally-averaged flow has been demonstrated nicely by the numerical experiment reported by Hoskins (1983; Fig. 7.4).

One of the interesting features in Fig. 3 is the tendency for the baroclinic and barotropic conversion terms to cancel each other to some extent over the storm tracks so that the net effect (Fig. 3c) in these regions has considerably smaller values than $C1^{BP}$. The largest positive values of $C1^{BP}$ and the largest negative values of $C2^{BP}$ are seen, from Fig. 3, to occur at almost the same place. At first this appears strange in light of the theoretical results by Simmons and Hoskins (1978), who performed a numerical experiment on the life cycle of a baroclinic disturbance. They demonstrated a baroclinic growth of a disturbance followed a few days later by a barotropic decay of the disturbance. On the basis of these results one might have expected the largest negative values of $C2^{BP}$ to be found a relatively long distance down-

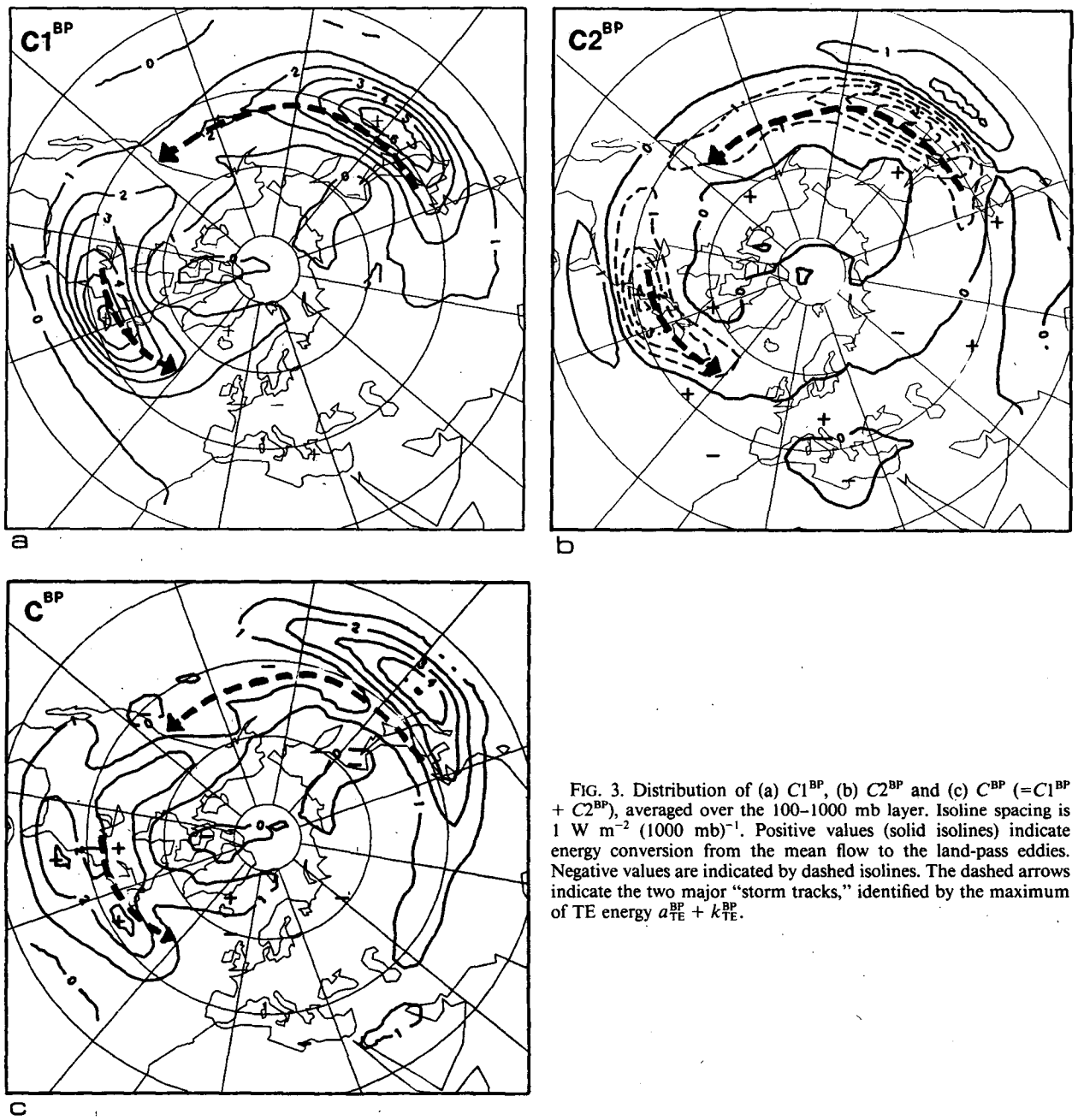

FIG. 3. Distribution of (a) $C1^{BP}$, (b) $C2^{BP}$ and (c) C^{BP} ($=C1^{BP} + C2^{BP}$), averaged over the 100–1000 mb layer. Isoline spacing is 1 W m^{-2} (1000 mb)$^{-1}$. Positive values (solid isolines) indicate energy conversion from the mean flow to the land-pass eddies. Negative values are indicated by dashed isolines. The dashed arrows indicate the two major "storm tracks," identified by the maximum of TE energy $a_{TE}^{BP} + k_{TE}^{BP}$.

stream (eastward) from the maximum of $C1^{BP}$. The probable explanation for this discrepancy is that much of the $C2$ conversion, but not $C1$ conversion, takes place eastward of the maximum of $C1^{BP}$ (minimum of $C2^{BP}$), and that it occurs at lower frequencies that are not captured by our band-pass filtering. Some support for this view is obtained from our results for low-pass eddies, discussed in Section 5. (Figure 5b shows, for example, that the low-frequency fluctuations experience a strong barotropic decay, $C2^{LP} < 0$, over the northeastern Pacific, east of the areas where Fig. 3 shows large band-pass energy conversions.)

The net energetic effect of the band-pass eddies on the time-mean flow is shown in Fig. 3c. It is seen to be dissipative ($C^{BP} > 0$) practically everywhere with largest dissipation taking place in the areas of the mean jet streams near the eastern coasts of the two continents.

A natural question that arises in connection with Fig. 3c is how the energy balance of the time-mean flow is maintained against the net dissipative effect

of the synoptic-scale eddies. The full treatment of this problem is beyond the scope of the present paper. It suffices here to note that this dissipation must, on the average, be compensated for by the work done by "residual" ageostrophic mean circulation, discussed, e.g., by Edmon *et al.* (1980) and Hoskins (1983). (Locally, flux divergence terms can also be significant.)

Reservations might be raised with respect to the significance of the present analysis in light of Plumb's (1983) comment that physical interpretation of individual terms in the energetics analysis normally depends upon the analysis scheme used, and that safe statements can be made only in respect to total contributions, i.e., the sum of all relevant conversion and flux divergence terms. This comment is a valid one, but the point to be emphasized here is that in the vertically integrated case, our C is effectively such a sum term, because it represents the net TE effect on the kinetic energy of the time-mean flow in the air column.

In light of the results shown in Fig. 3, the most essential effect of the synoptic-scale eddies is the decrease of the shear part and increase of the barotropic part of the time-mean flow over the storm track regions. One aspect of this phenomenon is, as demonstrated in B, westerly acceleration in the lower troposphere along the storm tracks.

4. Different methods of illustrating the TE effect on the time-mean flow

A question encountered in the verification and intercomparison of weather prediction and general circulation models is how to illustrate the interplay between the transient eddies and the time-mean flow. There are, in principle, several ways of doing this. Table 1 lists, in more or less chronological order, the methods used thus far for mapping the three-dimensional distribution of the TE effects.

Method 1 consists of mapping the TE fluxes (or flux divergences) of heat and momentum. It is the natural first choice and has been extensively used [see, e.g., the review in Holopainen (1983)]. In connection with this method, one should remember that for the TE mean flow interaction problem it is the divergent flux component that matters (Lau and Wallace, 1979); the nondivergent component is irrelevant. A fundamental deficiency of this method is that it does not account for the effect of TE induced secondary circulations.

Method 2 ("response method") requires solving some model of the time-mean circulation for the response to the TE fluxes of heat and momentum. Such a solution has ben worked out by Youngblut and Sasamori (1980) using a quasi-geostrophic model, and by Opsteegh and Vernekar (1982) using a primitive equation model. The results appear to be rather model-dependent. Therefore, this method cannot yet be used as a general method for the illustration of the net TE effects. Methods are needed which are more advanced than method 1 but simpler than method 2.

Method 3 (Holopainen *et al.*, 1982) is based upon mapping the divergent component of the TE flux of QGPV in the interior of the fluid. The drawback of this "q method" is that the divergent TE heat fluxes at the upper and lower boundaries should be shown

TABLE 1. Some diagnostic techniques of illustrating the regional distribution of the transient eddy (TE) effects on the time-mean flow.

Method characterization	Quantities to be mapped	Comments
1. Basic method	TE fluxes (or flux divergences) of heat and momentum (e.g., Lau *et al.*, 1981; Oort, 1983)	The role of the TE induced secondary circulations missing
2. Response method	Model response to the TE forcing given by method 1 (e.g., Youngblut & Sasamori, 1980; Opsteegh and Vernekar, 1982)	Results depend on the model and the mean flow used
3. q method	$(\overline{q'\mathbf{V}'})_D$ in the interior, $(\overline{(\theta'\mathbf{V}'})_D$ at the boundaries (Holopainen *et al.*, 1982)	In principle good, but boundary effects difficult to visualize
4. E method	Three-dimensional flux $E = \left(\overline{v'^2} - \overline{u'^2}, -\overline{u'v'}, \frac{f\overline{\theta'v'}}{\partial\bar{\theta}/\partial p}\right)$ (Hoskins *et al.*, 1983)	Compared with "q method", easier to apply but involves approximations
5. Tendency method	TE induced quasi-geostrophic initial tendencies (Lau and Holopainen, 1984)	Illustrates well the net TE forcing; tells nothing about the steady-state response
6. Energy method	$C1$ and $C2$ (the present paper)	An extension of "q method". Also takes into account the mean flow

simultaneously, and that the part of the TE forcing connected with the TE boundary heat fluxes is not necessarily easy for one to visualize.

The fourth method is an attempt to extend into three dimensions the Eliassen-Palm (EP) fluxes, which, since the study of Edmon *et al.* (1980), have been used extensively for demonstrating, in the mean meridional plane, the eddy mean-flow interaction and the propagation of the eddy activity. The "E method" by Hoskins *et al.* (1983) consists essentially of representing on the same map the geographical distribution of the TE meridional heat flux in the lower troposphere, taken to be an illustration of the generation of wave enstrophy, and of the anisotropy vector $[(\overline{v'^2} - \overline{u'^2})\mathbf{i} - \overline{u'v'}\mathbf{j}]$ in the upper troposphere. Compared with the "q method," the "E method" is easier to apply but involves approximations. Also, when the "E method" is used, the effects of the TE boundary heat fluxes are difficult for one to visualize.

With the fifth—the "tendency method" (Lau and Holopainen, 1948), the TE effects can be illustrated by the initial geopotential height tendencies (and/or the associated temperature and wind tendencies) which a quasi-geostrophic model atmosphere experiences if the TE fluxes of heat and momentum are switched on. This method appears to illustrate well the net TE forcing. However, as with all the other methods (except method 2), it tells nothing about the steady-state response to the TE forcing.

In this situation, with several advanced diagnostic techniques at hand, the comparison of the techniques is worthwhile and a few comments will be made in this respect. First, the "q method" and the "E method" will be compared concerning the way in which they picture the barotropic forcing of the time-mean flow. Then, a few words will be said about the similarities and dissimilarities of the "tendency method" and the "energy method."

Figure 4 shows three maps, all evaluated from the band-pass filtered NMC data, all having the same level of horizontal smoothing and referring to a vertical average [denoted by $\hat{(\ )}$] in the 100–1000 mb layer. Figure 4a shows the field $(\partial\hat{\bar{u}}/\partial t)_{TE}$ (E method) obtained as the vertically-averaged divergence of the vector $(\overline{v'^2} - \overline{u'^2})\mathbf{i} - \overline{u'v'}\mathbf{j}$. Figure 4b shows the distribution of $(\partial\hat{\bar{u}}/\partial t)_{TE}$ (q method), obtained as the zonal component of the vertically-averaged force $\mathbf{F}_{ND}^{VORT}$, which, in Fig. 4c, is pictured in a vectorial form with the aid of the associated streamfunction ($\mathbf{F}_{ND}^{VORT} = \mathbf{k} \times \nabla\Psi_{ND}^{VORT}$). Thus, both Figs. 4b and c refer to the "q method," the pattern in Fig. 4b being just the negative y derivative of the pattern in Fig. 4c.

Figures 4a and b, which one might expect to be identical, obviously have some common features. The most notable of these is the westerly acceleration of the zonal flow along the storm tracks. However, despite the same level of smoothing, there are differences between the two maps. These differences are partly connected with the fact that the TE induced force in this case is a horizontal vector, which can be described explicitly with the "q method" (see Fig. 4c). In the "E method," however, the meridional component of the vector is indirectly imbedded in the zonal component [see Hoskins *et al.* (1983) for details], and its role cannot be seen easily. However, as we mentioned previously, the "E method" is much easier to apply than the "q method."

In order to compare the "energy method" with the "tendency method," Fig. 3 in this paper, showing the patterns of $C1^{BP}$ and $C2^{BP}$, can be considered simultaneously with Fig. 3 in the Lau and Holopainen (1984) paper, which shows the initial geopotential height tendencies associated with the observed TE fluxes of heat and momentum in the band-pass eddies. Both figures are based on the same filtered NMC data. The tendency field illustrates in the storm track regions westerly acceleration in the lower troposphere and easterly acceleration in the upper troposphere due to the irrotational TE heat fluxes, and westerly acceleration at all levels due to the TE heat momentum fluxes. A decrease (increase) of the baroclinic (barotropic) component of the time-mean flow over the storm tracks is thus implied, a result which was also obtained by using the "energy method." The "tendency method" and the "energy method" are, thus, at least in this respect, compatible with each other, although they have a very different physical basis.

Methods 1, 3, 4 and 5 illustrate only the TE forcing field, which is determined by the TE variance and covariance fields. In the application of method 6, developed in this paper, information is also needed about the structure of the mean flow.

Further studies and intercomparisons are obviously necessary in order to find out the best technique of diagnosing the TE effects in a simple, yet quantitative and physically meaningful, way.

5. Some comments on the mean-flow effects arising from the transient eddies with periods between 10 and 90 days

In this paper, the main emphasis has been on the statistical effect of synoptic-scale (band-pass) eddies. However, if we deal with the climate problem, the longer-period fluctuations can be expected to play the dominant role in the eddy-mean flow interaction. Such fluctuations have recently received much attention (e.g., Wallace and Blackmon, 1983; Blackmon *et al.*, 1984). The low-pass NMC data represent fluctuations at periods from 10–90 days. It is now of some interest to consider the impact of these (LP) transient eddies on the climatological mean flow by applying the same technique as in the case of band-pass eddies.

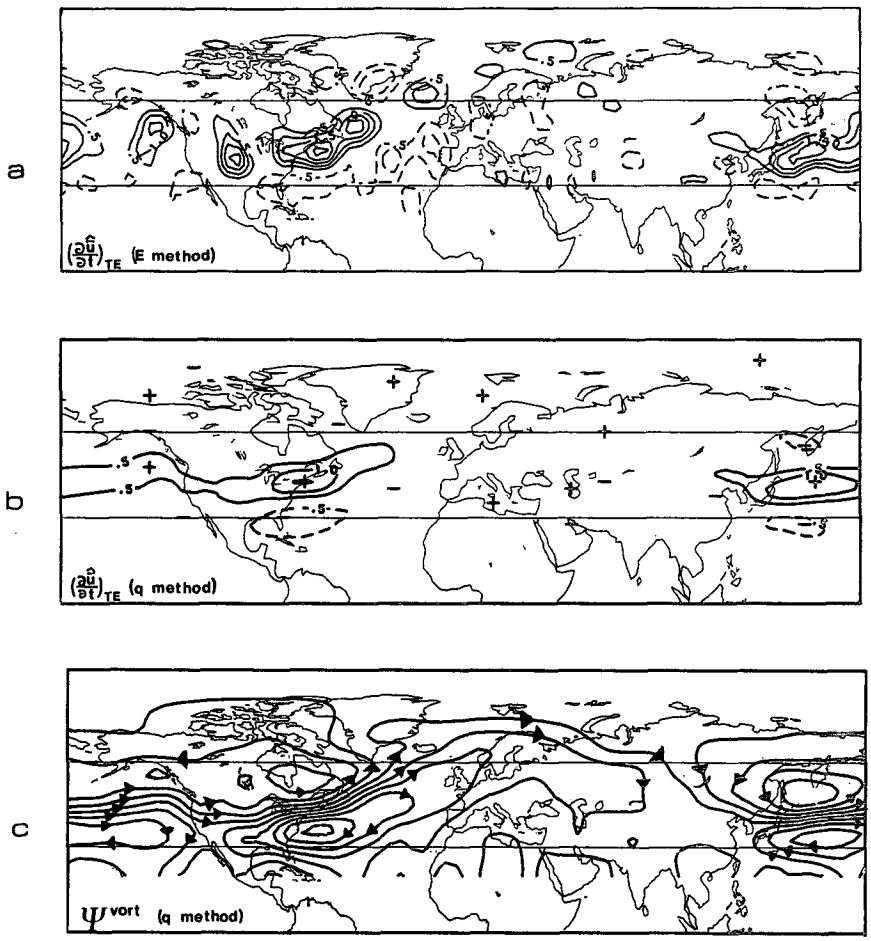

FIG. 4. Distribution of the local (BP eddy induced) acceleration of the vertically averaged zonal wind component, estimated by using (a) the "E method", and (b) the "q method"; isoline spacing 0.5×10^{-5} m s^{-2}. For the sake of clarity, the zero contour is not plotted. Panel (c) shows streamfunction Ψ^{VORT} for the vectorial force $\mathbf{F}_{ND}^{VORT}$ ($=\mathbf{k} \times \nabla\Psi^{VORT}$), the zonal component of which is seen in panel (b); isoline spacing: 2 m^2 s^{-2}.

The field of CA^{LP} (not shown) exhibits main maxima in the high latitudes and the values are positive practically everywhere. Thus, there is in the LP eddies as well, a conversion of the mean flow available potential energy to eddy energy with the domain average amounting to 1.5 W m^{-2} (1000 mb)$^{-1}$. While this conversion in the BP was determined primarily by the meridional heat fluxes over the storm track regions, in the LP eddies, a considerable part of it appears to be associated with the zonal TE fluxes (from the warmer oceans to the colder continents).

Averaged over the whole domain, the CK^{LP} term (map not shown) gives a conversion of the mean-flow kinetic energy to the LP eddies at the rate of 0.2 W m^{-2} (1000 mb)$^{-1}$. The climatological mean flow can thus be formally considered barotropically unstable with respect to these fluctuations. This is in accordance with the theoretical study of Simmons *et al.* (1983). The conversion appears to take place from the time-mean (stationary) eddies and not from the zonally-averaged time-mean flow, in qualitative agreement with a theoretical study by Lorenz (1972).

The patterns of $C1^{LP}$ and $C2^{LP}$ (which are different from those of CA^{LP} and CK^{LP}) are shown in Fig. 5. In contrast to the results for the BP eddies (Fig. 3), the two fields in Fig. 5 appear almost totally decoupled from each other and, thus, unlike the BP eddies, do not exhibit any tendency for the balance between baroclinic and barotropic conversion terms. The major maxima of $C1^{LP}$ occurs in the high latitudes, where large divergent downgradient heat fluxes in the LP eddies in winter take place from the warm oceanic areas to the relatively colder continental regions. The pattern of $C2^{LP}$ in Fig. 5b indicates that the low-frequency eddies receive kinetic energy from the climatological mean flow in the subtropics in the area of the mean jet streams, and feed it to the mean flow in the middle latitudes, particularly over the

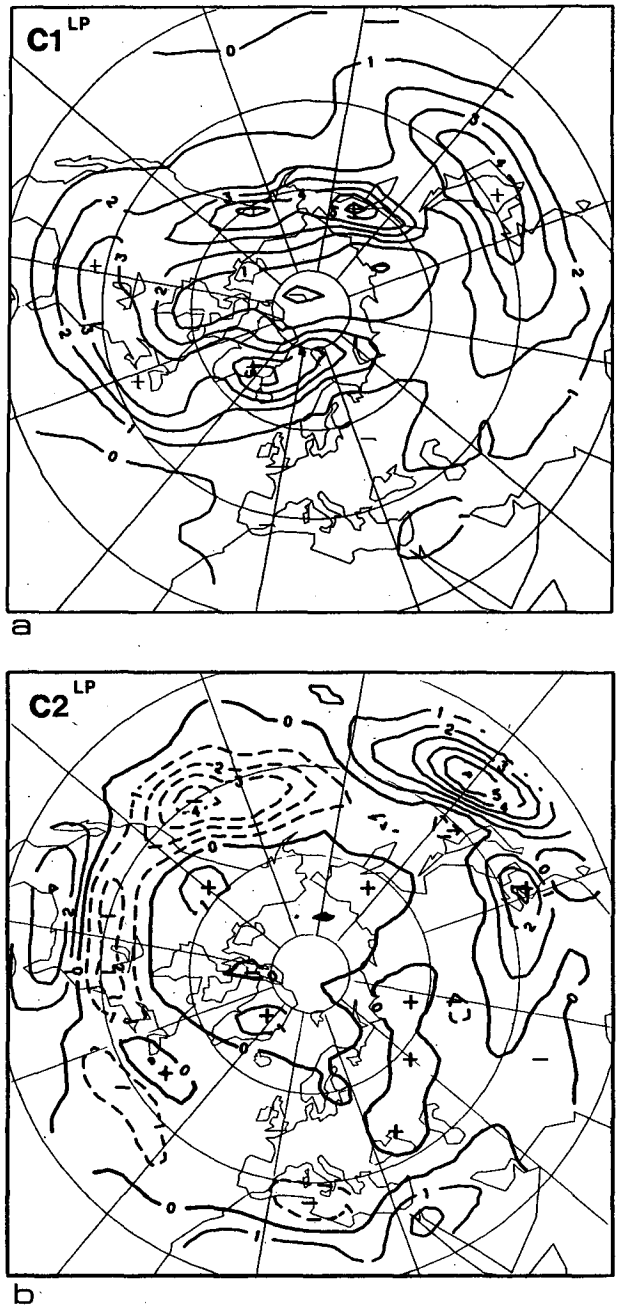

FIG. 5. As in Fig. 2 but for (a) $C1^{LP}$ and (b) $C2^{LP}$.

eastern Pacific, where the time-mean flow is rather weak. Thus, in addition to a small net conversion of the mean-flow kinetic energy to that of the LP eddies, the net effect is a tendency to shift the mean jet stream northeastward.

6. Summary

In this paper a new scheme has been presented for the illustration of the interplay between the time-mean flow and the large-scale transient eddies (TE). It is based upon the concept of the net work done in an air column by the mean nondivergent force which arises due to the TE fluxes of heat and momentum.

The main results of the present study are obtained when the new concept is applied to "synoptic-scale" eddies with periods between 2.5 and 6 days. It is shown that over the two major storm track regions, where these eddies have maximum intensity, there is a TE induced decrease (increase) of the baroclinic (barotropic) component of the time-mean flow.

A comparison of the proposed scheme with those suggested earlier for the illustration of the TE effects indicates that it could be a useful diagnostic tool in, for example, the verification and intercomparison of the synoptic-scale TE activity in the model atmospheres.

Acknowledgments. The author is indebted to Dr. N-C. Lau (Geophysical Fluid Dynamics Program, Princeton, NJ) for providing the NMC data used in this study, and to Mr. K. Ruosteenoja (Department of Meteorology, University of Helsinki) for the very capable data processing work. The comments by Drs. B. J. Hoskins, R. A. Plumb and G. H. White on the first version of the manuscript are gratefully acknowledged.

REFERENCES

Blackmon, M. L., 1976: A climatological spectral study of the 500 mb geopotential height of the Northern Hemisphere. *J. Atmos. Sci.*, **33**, 1607–1623.

——, Y.-H. Lee and J. M. Wallace, 1984: Horizontal structure of 500 mb height fluctuations with long, intermediate and short time scales. *J. Atmos. Sci.*, **41**, 961–979.

Bretherton, F. B., 1966: Critical layer instability in baroclinic flows. *Quart. J. Roy. Meteor. Soc.*, **92**, 325–334.

Edmon, H. J., B. J. Hoskins and M. E. McIntyre, 1980: Eliassen-Palm cross sections for the troposphere. *J. Atmos. Sci.*, **37**, 2600–2616.

Holopainen, E. O., 1978: A diagnostic study of the kinetic energy balance of the long-term mean flow and the associated transient fluctuations in the atmosphere. *Geophysica*, **15**, 125–145.

——, 1983: Transient disturbances in midlatitudes: observational aspects. *Large-Scale Dynamical Processes in the Atmosphere*, B. J. Hoskins and R. P. Pearce, Eds., Academic Press, 201–233.

——, L. Rontu and N-C. Lau, 1982: The effect of large-scale transient eddies on the time-mean flow in the atmosphere. *J. Atmos. Sci.*, **39**, 1972–1984.

Hoskins, B. J., 1983: Modeling of the transient eddies and their feedback on the mean flow. *Large-Scale Dynamical Processes in the Atmosphere*, B. J. Hoskins and R. P. Pearce, Eds., Academic Press, 169–197.

——, I. N. James and G. H. White, 1983: The shape, propagation and mean-flow interaction of large-scale weather systems. *J. Atmos. Sci.*, **40**, 1595–1612.

Lau, N-C., and J. M. Wallace, 1979: On the distribution of horizontal transports by transient eddies in the Northern Hemisphere wintertime circulation. *J. Atmos. Sci.*, **35**, 1844–1861.

——, and E. O. Holopainen, 1984: Transient eddy forcing of the time-mean flow as identified by geopotential tendencies. *J. Atmos. Sci.*, **41**, 313–328.

——, G. H. White and R. L. Jenne, 1981: Circulation statistics for the extratropical Northern Hemisphere based on NMC analyses. NCAR Tech. Note 171 + STR, 183 pp. [Available by request from NCAR, Boulder, CO.]

Lorenz, E. N., 1955: Available potential energy of the maintenance of the general circulation. *Tellus*, **7**, 157–167.

——, 1972: Barotropic instability of Rossby wave motion. *J. Atmos. Sci.*, **29**, 258–264.

Oort, A. H., 1964: On estimates of atmospheric energy cycle. *Mon. Wea. Rev.*, **92**, 483–493.

——, 1983: *Global Circulation Statistics 1958–1973.* NOAA Prof. Paper No. 14, 180 pp. [Available from U.S. Govt. Printing Off., Washington, DC 20402.]

Opsteegh, J. D., and A. D. Vernekar, 1982: A simulation of the January standing wave pattern including the effects of transient eddies. *J. Atmos. Sci.*, **39**, 734–744.

Pfeffer, R. L., 1981: Wave-mean flow interactions in the atmosphere. *J. Atmos. Sci.*, **38**, 1340–1359.

Plumb, A., 1983: A new look at the energy cycle. *J. Atmos. Sci.*, **40**, 1689–1708.

Simmons, A. J., and B. J. Hoskins, 1978: The life cycle of some nonlinear baroclinic waves. *J. Atmos. Sci.*, **35**, 414–432.

——, J. M. Wallace and G. W. Branstator, 1983: Barotropic wave propagation and instability, and atmospheric teleconnection patterns. *J. Atmos. Sci.*, **40**, 1363–1392.

Wallace, J. M., and M. L. Blackmon, 1983: Observations of low-frequency atmospheric variability. *Large-Scale Dynamical Processes in the Atmosphere*, B. J. Hoskins and R. P. Pearce, Eds., Academic Press, 55–94.

Youngblut, C., and T. Sasamori, 1980: The nonlinear effects of transient and stationary eddies on the winter mean circulation. Part I: Diagnostic analysis. *J. Atmos. Sci.*, **37**, 1944–1957.